

Critical Dynamics of Sound in KMnF_3

K. Fossheim and R. M. Holt

Department of Physics, University of Trondheim, The Norwegian Institute of Technology, 7034-NTH Trondheim, Norway

(Received 6 June 1980)

The critical dynamics of KMnF_3 above the cubic-tetragonal transition were studied by ultrasonics, including a novel phonon-echo technique. Well above T_c , the results confirm predictions obtained from the three-dimensional Heisenberg model, including the value of the crossover exponent $\phi=1.26$. Analysis of deviations from quasistatic behavior near T_c yields for the first time a dynamic scaling function $G(\omega\tau)$ for the critical attenuation of ultrasound. τ may be interpreted as the relaxation time of ordered clusters. We find that $\tau \approx 9 \times 10^{-13} t^{-1.41}$ s.

PACS numbers: 64.60.Ht, 62.65.+k, 63.75.+z

Critical attenuation of ultrasound at structural phase transitions has been studied in a number of systems over the last decade. Yet, even in the perovskites, which have been the subjects of numerous investigations,¹⁻⁶ several important questions of theoretical as well as experimental nature have remained. As examples of this we mention (i) the possibility of dimensional crossover^{4, 5, 7} in the temperature exponent ρ for the attenuation coefficient α , and (ii) the strong deviation from ω^2 dependence reported^{2, 4, 8} for the attenuation in KMnF_3 .

In the present Letter we focus on two items: (a) a new experimental technique (echo technique) capable of removing wave-front distortions occurring in soundwaves propagating in inhomogeneous media; (b) experimental results obtained or substantiated by this technique near the transition temperature $T_c = 187$ K in KMnF_3 , and their interpretation. Analysis of the results in relation to renormalization-group calculations⁹ leads for the first time to direct determination of a dynamic scaling function for ultrasonic attenuation near a structural phase transition.

Until now, the sample-quality problem has been a major obstacle in ultrasonic work near structural phase transitions. This problem arises from the fact that the sound velocity v is a strongly varying function of the relative temperature $t = (T - T_c)/T_c$. Since T_c will vary slightly with position \vec{r} in a nonperfect sample, v is also a function of \vec{r} , i.e., $v = v(\vec{r}, t)$ near T_c . Here, the conventional reflected pulse train is therefore often badly distorted by interference, rendering data inadequate for determination of critical exponents.

In the new ultrasonic technique, illustrated in the inset of Fig. 1, we have employed the electroacoustic echo effect.¹⁰ A forward acoustic pulse

of frequency ω and wave vector \vec{k} , $A_f \exp[-i(\omega t - \vec{k} \cdot \vec{r})]$, emitted as a plane wave from an acous-

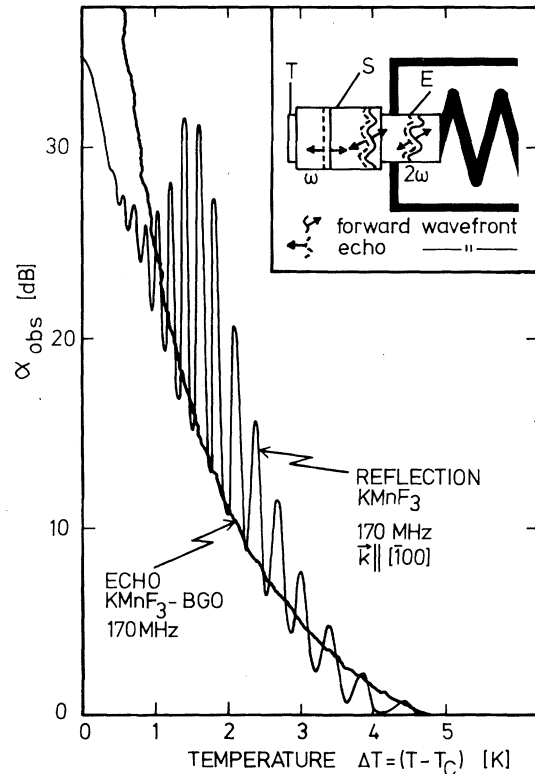


FIG. 1. Demonstration of (a) strong interference effects in a reflected pulse in a nonparallel sample of KMnF_3 recorded during a fast temperature sweep near T_c (thin line), and (b) removal of the interferences by echo technique (heavy line). The two curves were recorded *simultaneously*. Inset: Experimental configuration for echo investigation of KMnF_3 . The soundwave of frequency ω is generated by the transducer (T), transmitted through the sample (S), into the echo crystal (E) where it is exposed to the 2ω field of the spiral cavity. Wavefronts of forward wave (full lines) and backward wave (echo, broken lines) are illustrated.

tic transducer, is passed through the sample into the echo-active crystal bonded to it. For the present investigation we chose piezoelectric $\text{Bi}_{12}\text{GeO}_{20}$ (BGO) as the echo crystal. It is located in a microwave cavity tuned¹¹ to frequency 2ω . Here a homogeneous electric field $E = E_0 \exp(i2\omega t)$ is applied to the forward wave. By a mixing process, a backward acoustic wave $A_b \propto A_f E_0 \times \exp(i(\omega t + \vec{k} \cdot \vec{r}))$ is generated. The outcome of the mixing therefore is to *reverse* the wave vector, i.e., $\vec{k} \rightarrow -\vec{k}$, at all points on the wave front. The echo wave front now reconstructs continuously, replicating the original form during backward propagation, and finally reaches the transducer as a plane wave. At this stage a *correct* measurement of acoustic amplitude is made.

The technical improvements discussed above are demonstrated by measurements near T_c in KMnF_3 shown by the two curves of Fig. 1. A reflected pulse as well as the echo were recorded *simultaneously* and continuously during a fast temperature sweep in a nonparallel sample. While the reflection data display the resulting interference effects in a very pronounced manner, the echo shows no trace of it even under this extremely demanding test. Similar behavior is also seen close to T_c when the temperature is stabilized at each point and sample parallelism satisfies usual criteria. Thus the echo technique by \vec{k} reversal is capable of totally removing the interference effects caused by strong wave-front distortions.¹²

An important new aspect brought into the theoretical discussion of ultrasound by Murata⁹ is the crossover exponent ϕ entering in the critical exponent ρ for ultrasonic attenuation in perovskites. This exponent is introduced to account for the effective "spin" anisotropy due to the scaling field represented by the symmetry-breaking strain-order-parameter interaction terms in the Hamiltonian.^{13, 14}

The expression for the attenuation as given by Murata⁹ is

$$\alpha(\vec{k}, \mu) = [\omega^2 / 4M_c k_B T v^3(\vec{k}, \mu)] g(\vec{k}, \mu), \quad (1)$$

for a sound wave of wave vector \vec{k} and polarization μ . M_c is the unit-cell mass, k_B is Boltzmann's constant, T is the temperature, and $v(\vec{k}, \mu)$ is the sound velocity. The function¹⁵ $g(\vec{k}, \mu)$ as well as the exponents are different for different modes.

For each mode \vec{k}, μ , the function $g(\vec{k}, \mu)$ may be expressed as a sum of at most three terms:

$$g(\vec{k}, \mu) = \sum_{i=1}^3 \kappa_i(\vec{k}, \mu) K_i D_i^{2t - \rho_i},$$

where $\kappa_i(\vec{k}, \mu)$ are known¹⁰ mode-dependent numerical coefficients, K_i are⁹ derived from the four-point correlation functions for the F_g octahedra, and D_i are linear combinations of the coupling constants of the Hamiltonian.^{13, 14} The theoretical values⁹ for ρ_i are as follows in the $n=d=3$ Heisenberg model: $\rho_1 = 1.34$; $\rho_2 = \rho_1 + 2(\phi_2 - 1) = 1.86$; $\rho_3 = \rho_1 + 2(\phi_3 - 1) = 1.86$, with the crossover exponents $\phi_2 = \phi_3 = 1.26$.

Experiments were carried out using the following modes: L[100], L[110], T[110], and L[111]. All modes were studied by echo technique as well as by conventional pulse-reflection measurements.

The present investigation was far more extensive than any previously reported on this material. In particular the aim was to understand the strong deviations from ω^2 dependence reported earlier.^{2, 4, 8} It was necessary, therefore, to expand both the frequency range (15–700 MHz) and the temperature region ($0 < T - T_c < 30$ K) considerably relative to previous work. Furthermore, four separate samples were used. Samples I–III were of different origin (A. Linz, Massachusetts Institute of Technology) than sample IV (Centre d'Etudes Nucléaires, Grenoble). Data which are given in the figures below are mainly from sample IV, but the data from all samples are consistent.

It turned out that the expected ω^2 dependence could indeed be recovered by increasing the temperature sufficiently far above T_c . Also, in *this* range the exponents ρ_i took on values which were quite different from those reported by previous workers (with the one exception of Fosheim, Martinsen, and Linz,⁴ who studied ρ with $\vec{k} \parallel [100]$). The dominant exponent turned out to be very near 1.9, for *all* modes. This means that the weight factors $\kappa_i K_i D_i^{2t - \rho_i}$ favor terms containing the large ρ_i 's, i.e., ρ_2 and ρ_3 . Experimentally these cannot be distinguished. Measurements for the mode L[110] will be discussed in some detail below. At this point we note the fact that all results are consistent with $\rho_2 \approx \rho_3 = 1.87 \pm 0.05$, in close agreement with the predicted value⁹ of 1.86.

The typical behavior well above T_c for the important terms in the attenuation is hence

$$\alpha \sim \omega^{2.0 \pm 0.1} t^{-1.87 \pm 0.05} \quad (2)$$

based on measurements using four modes and four different specimens of KMnF_3 , of different origin and defect contents. The agreement with theory is striking. Further, it confirms the implied value of the crossover exponents $\phi_2 \approx \phi_3$

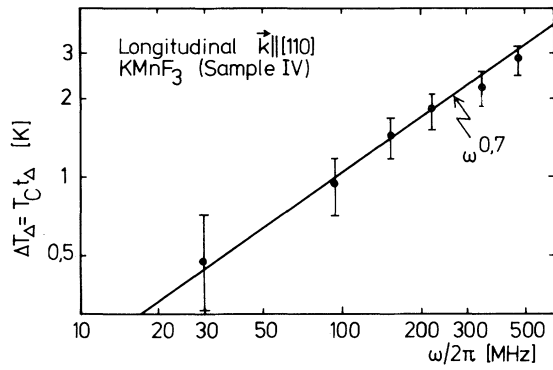


FIG. 2. Crossover temperature ΔT_{Δ} vs ω signaling the change from the hydrodynamic regime to the dynamical region closer to T_c in KMnF_3 . Data points are obtained from experiments, the full line corresponds to theoretical expectation as explained in the text.

≈ 1.26 , and constitutes the first determination of these exponents in KMnF_3 . A distinction between cubic and Heisenberg fixed points cannot be made since the difference is within experimental error.

However, as all data show, on approaching T_c the attenuation does *not* continue to diverge according to Eq. (2). Rather, a rollover is found: The frequency dependence is much weaker than ω^2 , and the ω exponent in some cases approaches unity very close to T_c .

To study this behavior the data were analyzed with respect to an, as yet, unknown dynamic scaling function¹⁶ $G(\omega\tau)$, i.e., we take

$$\alpha \sim \omega^2 t^{-1.87} G(\omega\tau), \quad (3)$$

where $G(\omega\tau)$ may be determined from a plot of $\alpha_{\text{obs}}/\omega^2 t^{-1.87}$ vs $\omega\tau$. $\tau = \xi^z = \xi_0 t^{-\nu z}$ is the relaxation time of correlated regions and ξ is the correlation length. The ultrasonic attenuation is not expected to exhibit singular behavior at the critical point except when $q=0$, $\omega=0$. This means that $G(\omega\tau)$ must have the following asymptotic form in the limit $\omega\tau \gg 1$:

$$G(\omega\tau) \sim (\omega\tau)^{-\rho/\nu z} = (\omega\tau)^{-1.32}.$$

In the opposite limit, $\omega\tau \ll 1$, we expect the usual scaling result such that $G(\omega\tau) = 1$.

The temperature-dependent time constant τ may be extracted by analysis of the crossover from quasistatic⁹ ($\omega\tau \approx 0$, $k\xi \approx 0$) to dynamic behavior ($\omega\tau \neq 0$, $k\xi \approx 0$). A plot of crossover temperature ΔT_{Δ} relative to T_c defined by the onset of the rollover is shown as a function of frequency in Fig. 2. The experimental points are taken to correspond to approximate fulfillment of the condi-

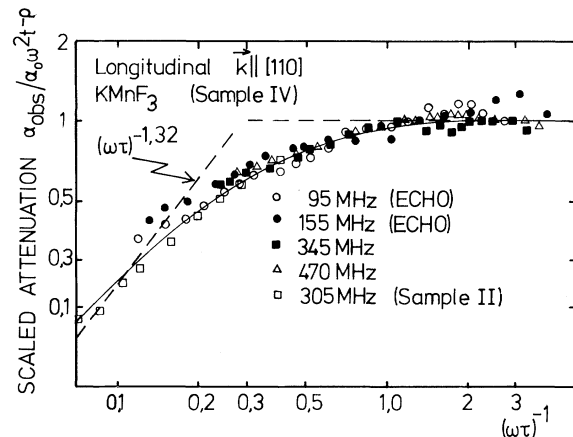


FIG. 3. Dynamic scaling function for ultrasonic attenuation in KMnF_3 determined by analysis of experimental data. The fully drawn curve represents the average of all data from a large number of frequencies with use of four different modes. Data points refer to one particular mode: $L[110]$. The dashed lines show the expected asymptotic behavior as discussed in the text. Because of the first-order character of the transition and corresponding uncertainty in T_c , the slope defined by the ~ 6 data points to the left is also somewhat uncertain.

tion $\omega\tau = 1$. The theoretically expected behavior can be deduced as follows.

The argument $\omega\tau$ of G may be written in the form $\omega\tau = (\omega/\omega_0) t^{-\nu z}$, where $z \approx 2$ is the dynamic scaling exponent as given in the relaxation model (model A of Halperin and Hohenberg¹⁶), believed to be the appropriate model for this system. The condition $\omega\tau = 1$ then corresponds to a crossover temperature $t_{\Delta} = (\omega/\omega_0)^{1/\nu z}$, where the exponent $1/\nu z$ in the three-dimensional Heisenberg model is 0.71. Such a line is drawn for comparison in Fig. 2. The agreement is quite good. This behavior rules out the possibility of dimensional crossover, since such a crossover would be frequency independent. The characteristic frequency ω_0 is also found: $\omega_0/2\pi \approx 1.8 \times 10^{11} \text{ s}^{-1}$, and the relaxation time in units of seconds is

$$\tau \approx 9 \times 10^{-13} t^{-\nu z}. \quad (4)$$

The function $G(\omega\tau)$ may now be deduced (Fig. 3). A simple result is found: $G(\omega\tau)$ is, within the limits of uncertainty, the same for all modes and samples. It approaches unity far from T_c , and, within the uncertainty it is in agreement with the predicted $(\omega\tau)^{-1.32}$ behavior close to T_c , as shown in Fig. 3. Note, however, that our data are not sufficiently accurate to determine whether

we are in the truly asymptotic region near T_c . This description replaces the previously suggested dimensional crossover.^{4,7} To our knowledge it represents the first determination of a dynamical scaling function for ultrasonic attenuation near phase transitions. In a recent paper by Suzuki,¹⁷ an attempt was made to include a dynamic scaling function in the expression for α in KMnF_3 . However, a determination of the scaling function was not achieved.

The time constant τ , which has been experimentally determined here, may be interpreted as the characteristic time of the cluster dynamics near T_c . Also, it may be seen as a direct manifestation of the inverse width of the central peak¹⁸ which is too narrow to be determined from neutron data.

The authors would like to acknowledge useful discussions with E. Pytte, G. Grinstein, and F. Schwabl, as well as comments from C. P. Enz.

¹B. Berre, K. Fossheim, and K. A. Müller, Phys. Rev. Lett. **23**, 589 (1969); K. Fossheim and B. Berre, Phys. Rev. B **5**, 3292 (1972).

²M. Furukawa, Y. Fujimori, and K. Hirakawa, J. Phys. Soc. Jpn. **29**, 1528 (1970).

³J. M. Courdille and J. Dumas, Solid State Commun. **9**, 609 (1971).

⁴K. Fossheim, D. Martinsen, and A. Linz, in *Anhar-*

monic Lattices, Structural Transitions and Melting, edited by T. Riste (Noordhoff, Groningen, 1974), p. 141.

⁵E. R. Domb, H. K. Schurmann, and T. Mihalisin, Phys. Rev. Lett. **36**, 1191 (1976).

⁶I. J. Fritz, Phys. Rev. Lett. **35**, 1511 (1975).

⁷F. Schwabl, Phys. Rev. B **7**, 2038 (1973).

⁸I. Hatta, M. Matsuda, and S. Sawada, J. Phys. C **7**, 2038 (1973).

⁹K. K. Murata, Phys. Rev. B **13**, 4015 (1976).

¹⁰R. B. Thompson and C. F. Quate, Appl. Phys. Lett. **16**, 295 (1970). For a technical demonstration of echo properties, see also for instance N. S. Shiren and R. L. Melcher, in *Phonon Scattering in Solids*, edited by L. J. Challis, V. W. Rampton, and A. F. G. Wyatt (Plenum, New York, 1976), p. 405.

¹¹K. Fossheim and R. M. Holt, J. Phys. **11**, 892 (1978).

¹²K. Fossheim and R. M. Holt, in Proceedings of the Third International Conference on Phonon Scattering in Condensed Matter, Providence, Rhode Island, August 1979 (to be published); R. M. Holt and K. Fossheim, Ferroelectrics **25**, 515 (1980).

¹³J. Feder and E. Pytte, Phys. Rev. B **1**, 4803 (1970).

¹⁴A. D. Bruce and A. Aharony, Phys. Rev. B **11**, 478 (1975).

¹⁵F. Schwabl (private communication) has redetermined the coefficients by mode-coupling calculations. Exponents ρ_i agree with Ref. 9.

¹⁶B. I. Halperin and P. C. Hohenberg, Rev. Mod. Phys. **49**, 435 (1977).

¹⁷M. Suzuki, J. Phys. C **13**, 549 (1980).

¹⁸In Ref. 8, estimates of the central peak width were also made. The data are in fair agreement. However, the existence of a dynamic scaling function $G(\omega\tau)$ was not revealed, and the critical exponent ρ was not determined in Ref. 8.